Streambank erosion and channel widening: implications for flood hazard

Adina Moraru

Supervised by
Virginia Ruiz-Villanueva (University of Geneva)
Glòria Furdada (University of Barcelona)

MSc in Mineral Resources and Geological Hazards
Specialty: Geological Hazards

Master thesis, July 2017

UNIVERSITAT DE BARCELONA

UAB
Universitat Autònoma de Barcelona

ABSTRACT

As one of the most threatening geological hazards, flash floods have noteworthy geomorphic effects (*e.g.* erosional and depositional modifications of the pre-event channel), hence, the main aim of this study was to provide an understanding of geomorphic indicators controlling channel widening during flood events. Floods over the past fifteen years affecting the uppermost areas of selected European rivers have been compiled in a database, subsequently completed and homogenized. Initial channel widths of 1.3m (Swiss Alps) to 217.27m (Apennines) showed channel widenings of 2.8% (Austrian Alps) to ~2000% (Apennines). Statistical analysis shows significant differences in channel widening among regions, depending on flood magnitude, catchment area, lateral confinement, and methodology used when gathering data. Slope gradient had great control over estimated hydraulic forces (*i.e.* stream power, stream power index, unit stream power) involved in river dynamics.

Keywords: Streambank erosion. Channel widening. Lateral confinement. Stream power. Database. Flood hazard.

RESUMEN

Las inundaciones relámpago, como uno de los riesgos geológicos de mayor amenaza para la población, tienen efectos geomórficos considerables, como pueden serlo las modificaciones del canal antes del evento. Por consiguiente, el principal objetivo de este estudio fue proporcionar conocimiento de los indicadores geomórficos que controlan el ensanchamiento del río durante una inundación. Episodios que afectaron durante los últimos quince años a las zonas altas de algunos ríos europeos seleccionados fueron recopilados en una base de datos, posteriormente completada y homogeneizada. Anchos iniciales de 1.3m (Alpes suizos) hasta 217.27m (Apeninos) mostraron ensanchamientos de 2.8% (Alpes austríacos) hasta ~2000% (Apeninos). El análisis estadístico revela diferencias significativas entre regiones, en función del periodo de retorno, el área drenante, confinamiento lateral y metodología empleada a la hora de recopilar los datos. El gradiente longitudinal del canal tuvo una influencia importante en los parámetros hidráulicos estimados (representativos de la energía de flujo), que regulan la dinámica aluvial.

Palabras clave: Erosión lateral. Ensanchamiento del canal. Confinamiento lateral. Energía de flujo. Base de datos. Peligro de inundaciones.

INTRODUCTION

River response to low frequency, high-magnitude floods can vary significantly, and a spectrum of controlling factors might influence this variation, with important impacts on its surrounding environment and population (Baker, 1988). Impacts of extreme floods have thoroughly been investigated, especially focusing on the geomorphic change during an episode: the amount of erosion and deposition (Krapesch *et al.*, 2011; Thompson and Croke, 2013), streambank erosion processes and channel widening (Piégay *et al.*, 2005; Bowen and Juracek, 2011; Krapesch *et al.*, 2011; Grove *et al.*, 2013; Buraas *et al.*, 2014; Magilligan *et al.*, 2015; Nardi and Rinaldi, 2015; Comiti *et al.*, 2016; Surian *et al.*, 2016), destruction of protection structures (Piégay *et al.*, 2005; Langhammer, 2010), etc. The documented variability of extreme flood effects reveals that floods of similar magnitude can result in impacts at a site over time and among sites (Hooke, 2015).
For a better understanding of channel dynamics and development of predictive tools that allow the assessment of temporal and spatial variations of geomorphic effects of high-magnitude floods, researchers investigated the possible driving forces to evaluate the ability of a flood to be geomorphologically effective and its capacity to modify channel morphology and forms over its duration (Costa and O'Connor, 1995; Magilligan *et al.*, 2015; Amponsah, 2017; Righini *et al.*, 2017).
The capacity to predict where large geomorphic changes occur during an extreme flood is still roughly poor considering the physical complexity and interdependent factors that control response magnitude and its spatial distribution (Buraas *et al.*, 2014). Studies support that prediction and understanding of channel and floodplain response to an infrequent flood should incorporate additional factors, such as river morphology, channel type, lateral confinement, vegetation cover, etc. (Piégay *et al.*, 2005; Langhammer, 2010; Thompson and Croke, 2013; Nardi and Rinaldi, 2015; Comiti *et al.*, 2016; Rinaldi *et al.*, 2016; Surian *et al.*, 2016; Amponsah, 2017; Righini *et al.*, 2017), besides the hydraulic forces (*i.e.* stream power, energy expenditure, velocity, discharge) traditionally considered.
Subsequently, it is of major importance forecasting spatial and magnitude variability of channel impacts as a result of the interaction of multiple potential controlling factors by means of i) recording the effects of extreme floods, ii) boosting flood hazard mapping in mountain rivers where this data is scarce; iii) providing tools that enhance a geomorphic approach to river management by outlining appropriate river strategies and planning, iv) improving risk mitigation in mountain rivers.

This thesis analyses the impacts of high-magnitude flood episodes in different European mountain rivers, and the role of certain variables in controlling morphological changes, not individually, as already investigated in previous works, but jointly, which enables us to provide an overview and to compare between episodes to highlight the importance of the main controlling factors of the processes ruling flood hazard.
The main objectives were:

i) to create a database of geomorphic and hydrologic characteristics of the selected study cases
ii) to assess streambank erosion and channel widening in selected study cases
iii) to provide an understanding of geomorphic indicators controlling channel widening during flood events

The final goal was to gather data and better knowledge that would help estimating potential widening-related hazards during floods.

STUDY SITES: THE RIVERS

In this study, nine recent flood events, which occurred during a time span of ten years (2005-2014), were analyzed in five regions, where a total of 54 watercourses (**Fig. 1**, **Table 1**) showed noticeable geomorphic changes. All of them are in an alpine context but the ones in Sardinia, where geology is of hercynian formation; all study sites are in the uppermost zones of the fluvial system, where erosion processes are predominant (Schumm, 1977; Rinaldi *et al.*, 2016). Detailed geologic context and further information about the rivers available in listed references. Slope gradient goes from $0.001 mm^{-1}$ (Swiss Alps and Spanish Pyrenees) to $1.05 mm^{-1}$ (Swiss Alps), initial width ranges from 1.30m (Swiss Alps) to 217.27m (Apennines), catchment area from less than $1 km^2$ in the Swiss Alps to over $650 km^2$ in Sardinia (see Database in **Electronic Appendix**).

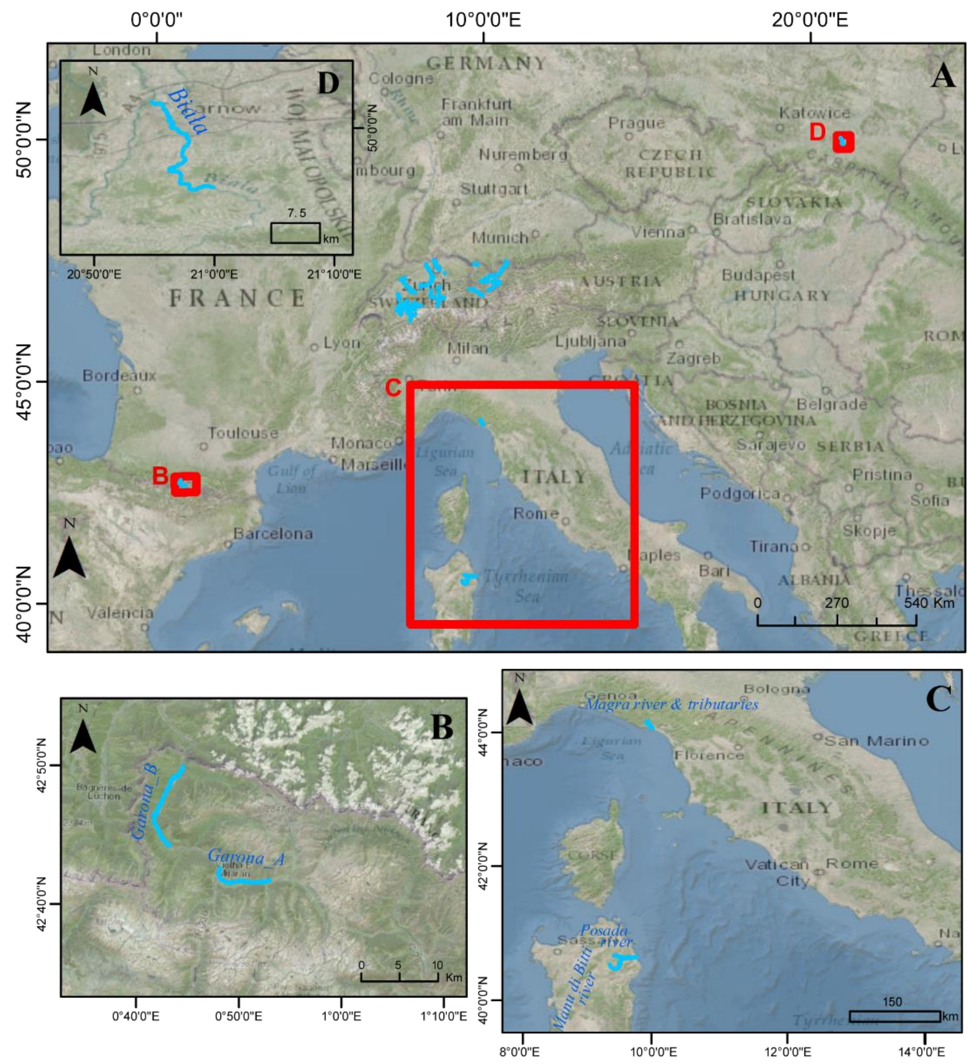

Figure 1. Study sites' location. A: general view, Alps in the center; B: Pyrenees; C: Apennines and Sardinia; D: Carpathians. Topographic base map' coordinates system: WGS84 Mercator Auxiliary Sphere (Esri [on line]).

Emme and other rivers in the Swiss Alps

Swiss Alps have been broadly affected by several floods during the past ten years (**Table 1**), therefore, a total of 43 watercourses in this region (*i.e.* Emme, Chirel, Kander, Lütschine, tributaries of these and Rhine and Reuss rivers, **Fig. 1A**) were considered. Return period (RT) ranges from frequent (30yr for Altibach river) to extreme (300yr for Emme and its tributaries, Badoux *et al.*, 2015), slopes from 0.001mm^{-1} to 1.05mm^{-1} (Ruiz-Villanueva *et al.*, *in progress*), catchment areas of less than 1km^2 or up to 345km^2 (Bachmann, 2012).

Garona (Pyrenees)

This river goes over the Spanish Pyrenees along 45km before reaching France and draining into the Atlantic Ocean (Confederación Hidrográfica del Ebro, CHE, 2008). Two detached stretches, of approximately 20km long altogether, were considered (*i.e.* study area A and B in Victoriano *et al.*, 2016; **Fig. 1B**). The 2013 flood affecting this watercourse, mainly caused by heavy rainfall (124.7mm in 48h in Vielha) and fast snow melting (40% of the flood discharge; Ros San Martin, 2015) was considered as one of a return period of ≤50years (CHE and Ministerio de Agricultura, Alimentación y Medio Ambiente, MAPAMA, 2014), with remarkable effects (*i.e.* Arties dam's breakage increased water level downstream; Victoriano, 2014).

Magra and its tributaries (Apennines)

Magra river and six of its tributaries (**Table 1**, **Fig. 1C**) were inundated in 2011 due to heavy rainfall (*e.g.* 326-500mm event accumulation maxima, Comiti *et al.*, 2016), with return periods of 100-300yr. Northern Apennines rivers showed initial widths of 3.00-217.27m, slope gradients of 0.003-0.206mm^{-1} and catchment areas of 0.7-33.8km^2. Lierza creek, in North Italy, was studied as well (Amponsah, 2017).

Biała (Carpathians)

Although the river is 102km-long, only sections along 20km in the Southeast of Poland (*e.g.* catchment area of 210km^2; **Fig. 1D**) were considered. Heavy rains (*e.g.* 200mm in 48h, 600m^3/s peak discharge, 80yr return period; Hajdukiewicz *et al.*, 2016) affected both unmanaged and channelized segments.

Other rivers in the Alps, Sardinia, etc.

Austrian watercourses near Switzerland (*e.g.* Alfenz, Bregenzerach, Lech, Rosanna, Trisanna, flooded in 2005; Krapesch *et al.*, 2011) and two streams in Sardinia, Italy (*e.g.* Posada and Manu di Bitti rivers, flooded in 2013; Amponsah, 2017; Righini *et al.*, 2017) were considered (**Table 1**; **Figs. 1A** and **1C**, respectively). Austrian Alps reaches were from 20 to 51km long, with catchment areas of 172-1211km^2 (Alfenz and Lech, respectively), initial river width of 12-80m, and slope gradients of up to 0.0246mm^{-1}, and a return period of 100 years. On the other hand, northeastern Sardinian rivers covered catchment areas of 302km^2 (Manu di Bitti) and 685km^2 (Posada river), semi-alluvial and alluvial channels, affected by shorter than 50 years return period events (Righini *et al.*, 2017).

Table 1. Selected reaches and sub-reaches recently affected by flood episodes, and the methodology used.

Flood date	Region	Main river	Affected reach/sub-reach	Methods	Data Reference
21-Aug-05	Alps	Lütschine	Schwartze Lütschine	Fieldwork, GIS	Hunzinger and Durrer, 2009; Bachmann, 2012
21-Aug-05	Alps	Chirel	Chirel	Fieldwork, GIS	Hunzinger and Durrer, 2009; Bachmann, 2012

Flood date	Region	Main river	Affected reach/sub-reach	Methods	Data Reference
21-Aug-05	Alps	Chirel	Fildrich	GIS	Bachmann, 2012
21-Aug-05	Alps	Kander	Chiene, Gornerewasser	GIS	Bachmann, 2012
21-Aug-05	Alps	Lütschine	Lütschine, Weisse Lütschine	Fieldwork	Hunzinger and Durrer, 2009
21-Aug-05	Alps	Kander	Kandertal, Kandersteg, Simme	Fieldwork	Hunzinger and Durrer, 2009
21-Aug-05	Alps	Emme	Emme, Ilfis, Trueb	Fieldwork	Hunzinger and Durrer, 2009
21-Aug-05	Alps	Rhine	Landquart	Fieldwork	Hunzinger and Durrer, 2009
21-Aug-05	Alps	Reuss	Reuss, Engelberger Aa, Grosse Melchaa, Kleine Emme, Muota, Isitalerbach, Chärstelenbach,	Fieldwork	Hunzinger and Durrer, 2009
28-Aug-05	Alps	Alfenz	Alfenz	GIS	Krapesch *et al.*, 2011
28-Aug-05	Alps	Bregenzerach	Bregenzerach	GIS	Krapesch *et al.*, 2011
28-Aug-05	Alps	Lech	Lech	GIS	Krapesch *et al.*, 2011
28-Aug-05	Alps	Rosanna	Rosanna	GIS	Krapesch *et al.*, 2011
28-Aug-05	Alps	Trisanna	Trisanna	GIS	Krapesch *et al.*, 2011
04-Jun-10	Carpathians	Biała	Biała	Fieldwork	Hajdukiewicz *et al.*, 2016
04-Jun-10	Alps	Heubach	Heubach, Murtengraben, Schlattgraben	Fieldwork	Bachmann, 2012
04-Jun-10	Alps	Chalberhönibach	Chalberhönibach	Fieldwork	Bachmann, 2012
10-Oct-11	Alps	Lonza	Lonza	GIS	Bachmann, 2012
10-Oct-11	Alps	Kander	Kander	GIS	Bachmann, 2012
10-Oct-11	Alps	Kander	Simme	Fieldwork	Bachmann, 2012
10-Oct-11	Alps	Lütschine	Weisse Lütschine	Fieldwork	Bachmann, 2012
10-Oct-11	Alps	Altibach	Altibach	Fieldwork	Bachmann, 2012
10-Oct-11	Alps	Glatt	Glatt	Fieldwork	Bachmann, 2012
25-Oct-11	Apennines	Magra	Magra, Gravegnola, Pogliaschina, Osca, Mangiola, Geriola, Teglia	GIS	Comiti *et al.*, 2016; Surian *et al.*, 2016; Amponsah, 2017

Flood date	Region	Main river	Affected reach/sub-reach	Methods	Data Reference
18-Jun-13	Pyrenees	Garona	Garona A, B	GIS	This project
18-Nov-13	Sardinia	Posada	Posada, Manu di Bitti	GIS	Amponsah, 2017
24-Jul-14	Alps	Emme	Emme, Leimbach, Buembachgrabe, Schöniseibach, Gärtelbach, Sädelgrabe, Bärselbach,	GIS	Ruiz-Villanueva *et al.*, *in progress*
02-Aug-14	Apennines	Lierza	Lierza	GIS	Amponsah, 2017

MATERIAL AND METHODS

Methodology followed in this thesis is summarized in **figure 2**. Morphological channel changes in response to the studied flood events were analyzed and quantified by field surveys and interpretation of aerial photographs in previous works performed in all the studied rivers, and further completed during this thesis by new GIS data generation in the Garona river (Spanish Pyrenees). The data was overall statistically analyzed in order to determine the significant controlling factors of channel widening.

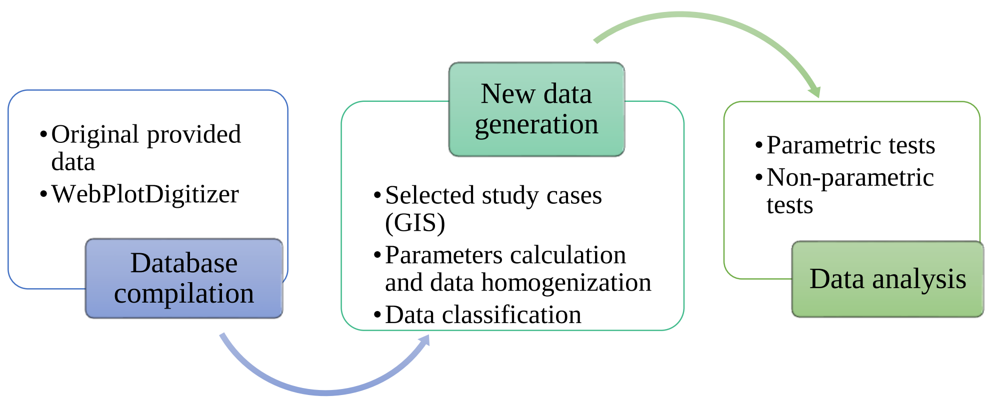

Figure 2. Methodology flow chart summary.

a. Compilation of a database of flood events, morphometric and hydrologic data of drainage basins, especially streambank erosion and channel widening

Pre- and post-flood data surveys were performed in different channel reaches along the studied watercourses: in the Alps (Hunzinger and Durrer, 2009; Krapesch *et al.*, 2011; Bachmann, 2012; Badoux *et al.*, 2015; Cavalli *et al.*, 2017; Rickenmann *et al.*, 2016; Rickli *et al.*, 2016;), the Apennines (Rinaldi *et al.*, 2012, 2013, 2015, 2016; Nardi and Rinaldi, 2015; Comiti *et al.*, 2016, Surian *et al.*, 2016, Amponsah, 2017, Righini *et al.*, 2017), Sardinia (Amponsah, 2017; Righini *et al.*, 2017), the Carpathians (Hajdukiewicz *et al.*, 2016) and the Pyrenees (CHE, 2008, 2013; Godé *et al.*, 2013; CHE and MAPAMA, 2014; Victoriano, 2014; García-Silvestre, 2015; Ros San Martin, 2015; Victoriano *et al.*, 2016). The observations included an analysis of geomorphic flood effects (as planimetric changes), an inventory of artificial structures (*i.e.* bank protection, dykes, channeling structures), and a qualitative assessment of the main morphological channel characteristics. This will be further explained in the following section b.

For the present investigation, data of flood events was gathered in a database. Original data was partially provided concerning the episodes in the Swiss Alps (Hunzinger and Durrer, 2009; Bachmann, 2012), Carpathians (Hajdukiewicz *et al.*, 2016), Pyrenees (CHE, 2013; Victoriano 2014; García-Silvestre, 2015; Ros San Martín, 2015), Apennines and Sardinia (Amponsah, 2017). When the original data was only available in published scatterplots, this was extracted semi-automatically using the online tool WebPlotDigitizer (Rohatgi, 2015). This tool was used for some parameters in the Austrian Alps (Krapesch *et al.*, 2011) and Apennines (Comiti *et al.*, 2016; Surian *et al.*, 2016). Once the data was compiled, parameters not available in former works, but feasible to estimate (*i.e.* unit stream power, stream power index, lateral confinement index, width ratio), were calculated in order to complete the database for further analysis.

b. New data generation by aerial photography and GIS analysis

Aiming to have a broader database, new data was generated in Garona river (Pyrenees). On that account, it was attempted to quantify and interpret some of the morphological characteristics, further described as it follows, as they could have an influence on bank erosion processes and, therefore, on the river's width (Nardi and Rinaldi, 2015). The study of morphological features is key to better understand the processes in charge of channel changes.

Regarding to making the data statistically comparable, the data generation process focused on the same aspects observed in previous works. Thus, these main parameters were digitized and calculated in pre- and post-flood aerial photographs and Digital Elevation Model (DEM) with ArcGIS 10.3.1 (see Methods in **Electronic Appendix**): active channel width, alluvial plain width, channel slope gradient, lateral confinement (LC), channel bed type, river type, artificial structures (*i.e.* bank protection, dykes, channeling structures), and vegetation cover. This was performed in two areas in Garona river, where the availability of high-resolution pre- and post-flood satellite images enabled a comprehensive assessment of potential change in channel width. Channel widening was represented in terms of width ratio (the ratio of channel width after the flood to channel width before the flood; Krapesch *et al.*, 2011).
This step contributed to criteria and expertise acquisition. A classification of the obtained data into different sub-sets (**Table 2**) allowed a simplified qualitative assessment of the main morphological channel characteristics (*i.e.* planimetric changes, confinement index) and the inventory of artificial structures, vegetation cover, river type, etc. This qualitative knowledge, that helps to interpret results, cannot be achieved just working with the quantitative data.

- Data generation and classification

The 2013 flood affecting the Garona river in the Spanish Pyrenees could be studied based on already existing data of both pre-event (ICGC, 2011 [on line]) and post-event (ICGC, 2013 [on line]) aerial photography (Victoriano, 2014; García-Silvestre, 2015), and further completed by GIS analysis. To study the significant geomorphic features, and focus on the notably affected areas in terms of flood effects, two detached stretches were selected (*e.g.* study area A and B in Victoriano *et al.*, 2016), of approximately 20km long altogether.

The new data acquirement process (see step by step in Methods in **Electronic Appendix**) begun with the mapping of the geomorphic features above mentioned, which was performed using geographic information systems (GIS) software (ArcGIS 10.3.1). This was applied to a set of high resolution pre- (*i.e.* pixel size of 25cm, a digital elevation model, DEM, with a 2-m spatial resolution; ICGC, 2011) and post-flood (*i.e.* pixel size of 22cm, a DEM with a 1-m spatial resolution; ICGC, 2014) satellite images (ICGC, 1956, 2011, 2013, [on line]) suitable for the study purpose, as the pixel size was sufficiently smaller than the river size and appropriate for identification of the features of interest.

Once the pre- and post-event active channels, as well as the alluvial plain, were digitized, and verified that the pre-event active channel was contained in the post-event channel and alluvial plain polygons, the centerline (Dilts, 2015) of the 2011 active channel polygon was used as a guide along which the survey points will be plotted. The two reaches were further partitioned into several transects regularly spaced at 50m intervals automatically drawn with the Transect Tool (Ferreira, 2014). The transects, perpendicular to the main flow direction, of a length larger than the alluvial plain's width, allowed to split the reaches into sub-reaches of minimum length as to extract a DEM-derived slope gradient of an adequate quality for stream power (SP) estimation (see section a.). These transects and the centerline were used as survey points where it was automatically calculated the pre- and post-event channel and alluvial plain's widths, catchment area (MAPAMA, 2006; QVI Inc., 2010; Roux *et al.*, 2015), channel lateral confinement, presence of artificial features, establishing vegetation classes, as well as the aforementioned slope gradient and unit stream power (USP) calculation (Rinaldi *et al.*, 2016; Righini *et al.*, 2017).

A numeric code was used to identify segments (*i.e.* assigned ID), however, the sub-reaches were named after the river they belonged to according to the original labelling (*i.e.* study area A and B, Victoriano *et al.*, 2016). The sub-reach scale allows analyzing the variability in channel response within the same stream, which might explain some expected localized off-the-regression-tendency results (see Results).

Active channel included low-flow channels and unvegetated or sparsely vegetated exposed sediment bars (Czuba *et al.*, 2012; Nardi and Rinaldi, 2015; Comiti *et al.*, 2016; Rinaldi *et al.*, 2016; Surian *et al.*, 2016). The changes in channel width were conveyed as the width ratio, Wr (*i.e.* channel width after divided by the channel width before the flood, as defined in Krapesch *et al.*, 2011).

Alluvial plain width included the present floodplain and low terraces, these considered as surfaces that can be a few meters more elevated than the floodplain and with the potential of being oddly flooded (Surian *et al.*, 2016; Righini *et al.*, 2017). The alluvial plain width was used to calculate the confinement index (C.I. = alluvial plain width / pre-event channel width, Comiti *et al.*, 2016) for the studied reaches.

Channel centerline was delineated by a semiautomatic process where the equidistant line from channel boundaries calculated every meter was extracted using the Polygon to Centerline Tool for ArcGIS (Dilts, 2015). This approach was also employed to define the channel slope gradient based on Digital Elevation Model (DEM) analysis by the Hydrology tool available in ArcGIS. Three slope classes (**Table 2**) were defined in order to ease data analysis: low (<0.02m/m), moderate (0.02-0.04m/m) and high (>0.04m/m), as in Rinaldi *et al.* (2012).

Table 2. Classes established in order to make the data analysis systematic, where NA: does not apply.

Parameter/Class	0	1	2	3
River morphology[1]	NA	Meandering	Braided	Straight
Slope gradient[2]	NA	Low	Moderate	High
Vegetation cover[1]	NA	Trees	Bushes	None/Other
Catchment area	NA	Small	Moderate	Large
Lateral confinement[2]	NA	Low	Moderate	High
Return period	NA	Frequent (<50yr)	Extraordinary (50-100yr)	Extreme (>100yr)
Embankment[3]	Natural	Partially constrained	Constrained	NA
Channel type[4]	NA	Bedrock	Semi-alluvial	Alluvial
Afforested area	NA	<40%	40-60%	>60%

[1]Bachmann, 2012, [2]Rinaldi *et al.*, 2012, [3]Hajdukiewicz *et al.*, 2016, [4]Righini *et al.*, 2017

Lateral confinement, expressed by the confinement index calculated as the alluvial plain width divided by the pre-event channel width (Rinaldi *et al.*, 2012, 2013; Thompson and Croke, 2013; Comiti *et al.*, 2016, Righini *et al.*, 2017), reflects the natural channel's lateral constraint and its potential lateral mobility. Rinaldi *et al.* (2012, 2013) classified this in three settings (**Table 2**) depending on the C.I. value: high confinement if 1-1.5, medium confinement if 1.5-5 and low confinement if this value surpassed C.I.= 5. However, in this study, these classes were defined as confined, partly confined, and unconfined rivers, respectively.

Three types of exposed bedrock were defined, *i.e.* bedrock (with 50-100% of exposed bedrock), semialluvial (mixed alluvial-bedrock, with 10-50% of exposed bedrock), and alluvial (with less than 10% of exposed bedrock) rivers (**Table 2**), as they were observed to alternate over short distances along the watercourse (Hajdukiewicz *et al.*, 2016; Righini *et al.*, 2017).

Bank protection (also called "embankment" in this thesis), dykes and channeling structures were either very restricted before the flood episodes (Bachmann, 2012; Comiti *et al.*, 2016; Righini *et al.*, 2017) or not considered in the analysis, as there is a lack of data in most studied cases. For the Garona river, an inventory of artificial structures was compiled based on a visually-skilled interpretation of aerial photographs before the flood occurred (ICGC, 2011 [on line]).

Same process was performed for the vegetation analysis, where three cover types were defined (*i.e.* forest was assigned type 1, bushes cover was type 2, and no vegetation/other was type 3; as in Bachmann, 2012). The afforested area was split in three sets depending on the proportion it covered (**Table 2**).

Rhoads (1987) defined stream power as a measure of geomorphic effectiveness of floods, as it quantifies river energy dissipation in alluvial systems. Stream power (SP, Ω) in originally provided data was calculated using the equation presented by Knighton (1999):

$$\Omega = \gamma \, Q \cdot S$$

where Ω is stream power (W/m), γ is the specific weight of water ($9810 N/m^3$), Q is the flood peak discharge (m^3/s), and S is channel slope gradient (m/m). Unit stream power (USP, ω, W/m^2) was calculated based on the equation presented by Bagnold (1977) as it follows:

$$\omega = \gamma\, Q \cdot S / W$$

where the parameters of the stream power equation are maintained, and W is the channel width measured before the flood (m). This parameter may be calculated both before and after the episode (Amponsah, 2017). As peak discharge values were not always available, hence, a stream power index (SPI) was used as a proxy instead. Stream power index was estimated by the following equation:

$$SPI = A\ (km^2) \cdot \gamma\ (N/m^3) \cdot S\ (m/m) / W\ (m)$$

where stream power index is presented in W/m^2, and A is the catchment area.

c. Statistical analysis of controlling factors to explain channel widening due to streambank erosion during floods

Most of the before mentioned factors are affected by significant observational uncertainties and can be undermined by theoretical errors (Amponsah, 2017), which should be considered together with the important uncertainties in the geomorphic response to high-magnitude floods.

A first analysis of the data (n=2539) consisted of simple regressions performed between channel widening (expressed as width ratio, Wr), and individual morphological and hydraulic variables on the entire data set at a sub-reach scale. Width ratios were compared among rivers using both parametric (*i.e.* simple regressions) and non-parametric (*i.e.* boxplots, Wilcoxon, Kruskal-Wallis) tests where appropriate (Clément and Piégay, 2003; Crawley, 2013). Statistical analyses were run on Software R (version 3.4.0) and Microsoft Excel (version 2016), with significance set at $p<0.05$.

Afterwards, simple regression was performed considering the same variables on different watercourses grouped as a function of channel bed type (*i.e.* bedrock, semi-alluvial and alluvial channels), vegetation cover class, river morphology, etc. (**Table 2**). These classes were set based on frequency histograms, as they showed evident breaks at certain values (*i.e.* 10 and $100km^2$ of catchment area), therefore these were selected as thresholds to distinguish parameter types or groups. Non-parametric Kruskal-Wallis, or Wilcoxon where pertinent, test of variance was used to determine the significance of differences between the several groups created according to the morphological characteristics listed above.

RESULTS

Once the database was compiled, the data gathered by previous individual studies was compared and only further analysed when the dataset was large enough as to perform statistical tests to it. Therefore, first, a general overview of the flood effects by region is presented in the table Statistical Summary (**Electronic Appendix**). The total amount of data (n=2539) considered is mentioned in each case (see Scatterplots and Boxplots in **Electronic Appendix**).

In a second step, an analysis of the following controlling factors was carried out in the overall database: width ratio depending on the studied region, the return period of the flood event, catchment area of the affected watercourses, lateral confinement, methodology used to gather the data, vegetation cover near the channel, slope gradient, embankment, river morphology and their impact in slope-dependent parameters, as stream power, unit stream power or stream power index.

Changes in channel width: width ratio

One of the main contributions of this study is an overview of the overall data, instead of analyzing the geomorphic effects of the study cases at a local scale. By comparing channel widening data (*i.e.* in terms of width ratio) significant differences between channel width changes depending on the region where the flood occurred (**Fig. 3**, right) were glimpsed. Alps and Carpathians showed lower width ratios than Sardinia and the Apennines, being the latter ones nearly twice as large, whereas Pyrenees showed intermediate values. Variability is notably broader in the Apennines than in any other of the considered regions. Kruskal-Wallis hypothesis contrast test indicates significant differences among the rivers (**Table 3**).

Width before event plotted against river's region (**Fig. 3**, left) reveals markedly higher initial channel widths in the Carpathians than in any other region, probably due to the lack of artificial structures or a lower lateral confinement. This will be further discussed later. Apennines had the smallest widths before the flood, although their and Carpathians' variances are the broadest. Alps, Pyrenees and Sardinia present alike values, but Sardinia has the smallest variance and the Alps the largest. Summary data as well as a scatterplot representing width ratio against stream power index are available in the **Electronic Appendix**.

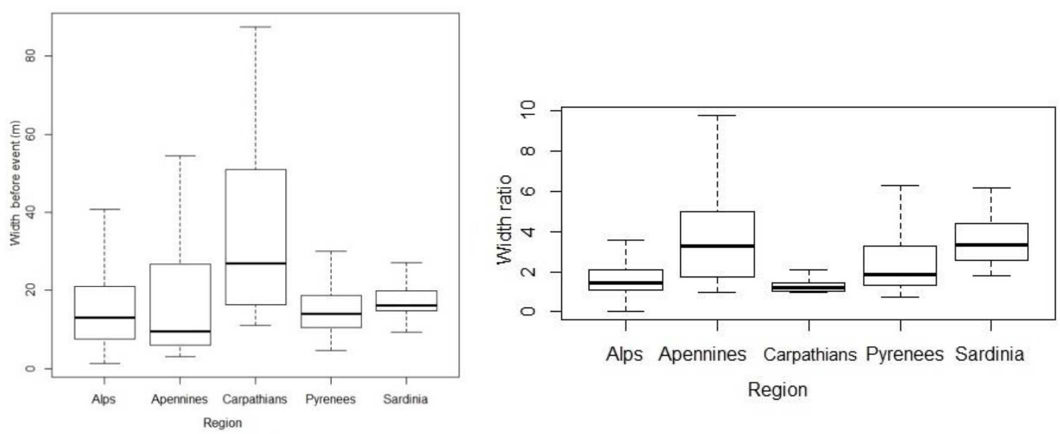

Figure 3. Left: boxplot representing channel width before event (m) against the region the river passed by the study area. Right: boxplot representing the width ratio against the rivers' region.

When representing width ratio against stream power index (SPI, hydraulic force dependent of the slope gradient, catchment area and width before the event; **Electronic Appendix**), it was observed that Apennines showed lower SPI but higher width ratio, with very little dispersion, whereas the Pyrenees or the Alps displayed larger SPI for low width ratios, and a more disperse tendency.

Flood magnitude and channel widening

Non-parametric hypothesis contrast tests (boxplot, **Fig. 4**, left; Kruskal-Wallis) show significant differences among the three flood return period classes, with larger median and variance for frequent floods (**Table 3**). Parametric testing (scatterplot, **Fig. 4**, right) shows a negative correlation between the initial channel width (Wbf) and width ratio (Wr) the lower the return period is. Scatterplots representing width ratio against stream power, unit stream power, and stream power index are available in the **Electronic Appendix**.

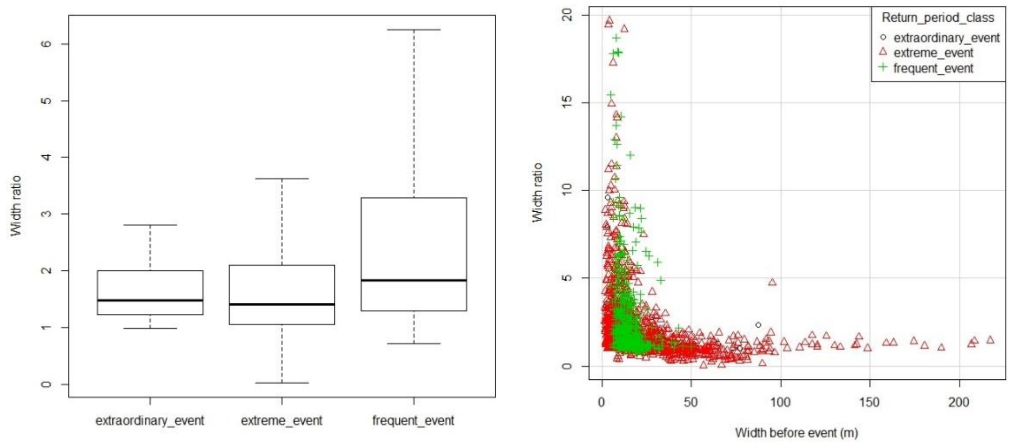

Figure 4. Left: boxplot representing width ratio against the return period class in the overall study sites. Right: scatterplot (n=2352) representing the width ratio against width before the event by the return period class (**Table 2**).

Catchment area and channel widening

Non-parametric hypothesis contrast tests (boxplot, **Fig. 5** left; Kruskal-Wallis) show significant differences among the three catchment area classes (**Table 3**), where river with large catchment areas suffered larger channel widening. However, larger catchment areas show a higher variability compared to moderate and small catchments. Krapesch *et al.* (2011) noticed that small sized catchment areas tend to have larger width ratios. Scatterplot in **figure 5** (right) shows that this trend is not necessarily followed only by small catchment areas. Scatterplots representing width ratio against width before the event is available in the **Electronic Appendix**.

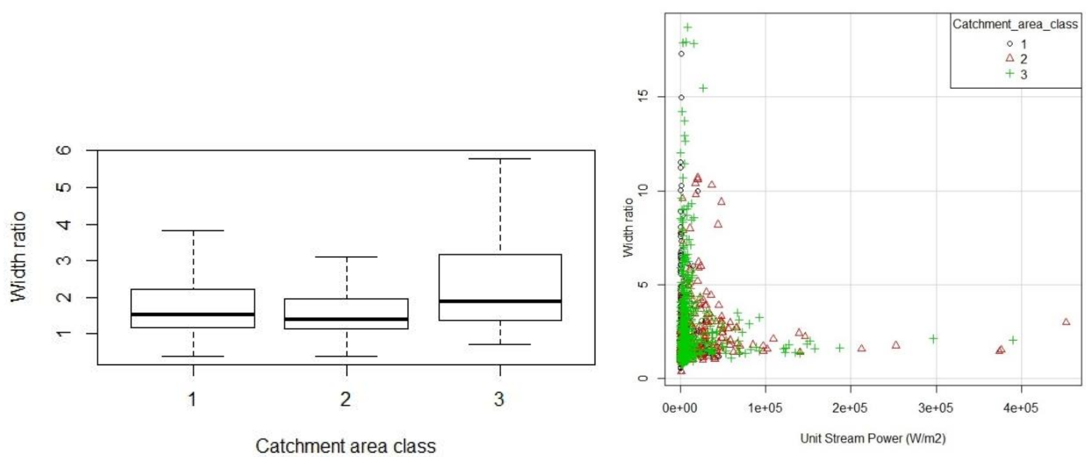

Figure 5. Left: boxplot representing width ratio against the catchment area class in the overall study sites. Right: scatterplot (n=1642) representing the width ratio against unit stream power (W/m^2) by the catchment area class (1: <10km; 2: 10km-100km; 100km <3, **Table 2**).

Lateral confinement and channel widening

Parametric testing (scatterplot, **Fig. 6**, right) reveals that watercourses with low confinement indexes (LCI) present a broader range of width ratios for similar stream power indexes. This is confirmed by non-parametric hypothesis contrast tests (boxplot, **Fig. 6** left; Kruskal-Wallis), which show significant differences among the three lateral confinement classes (**Table 3**): low LCI rivers suffer larger channel widenings, although the variability among rivers is remarkable. Scatterplots representing width ratio against width before event, stream power, unit stream power, as well as boxplots comparing slope and stream power index against the lateral confinement class are available in the **Electronic Appendix**.

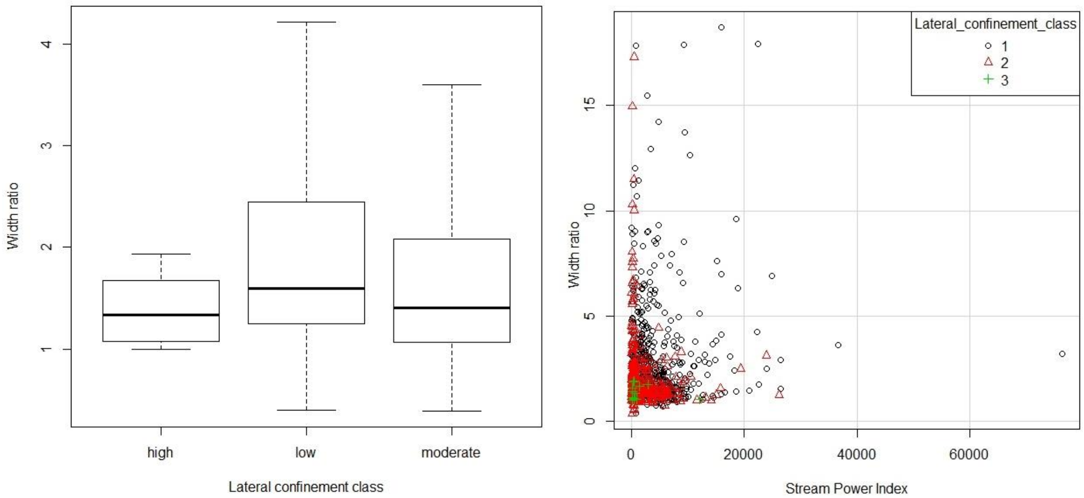

Figure 6. Left: boxplot representing width ratio against the lateral confinement class in the overall study sites. Right: scatterplot (n=1619) representing the width ratio against stream power index by the lateral confinement class (1: low; 2: moderate; 3: high, **Table 2**).

Type of methodology used in data acquisition and channel widening

Non-parametric (boxplot, **Fig. 7**, right; Wilcoxon) hypothesis contrast test show significant differences among the two methodology classes (**Table 3**). Scatterplots representing width ratio against stream power, unit stream power, and stream power index, as well as boxplots comparing lateral confinement index, slope gradient, stream power, stream power index, unit stream power and width before event against the methodology used are available in the **Electronic Appendix**. Plotting fieldwork and GIS data by their coordinates (**Fig. 7**, left), allows to confirm that measures were taken in the same spot. Non-parametric Wilcoxon test was applied to this episode's data, and it suggested that there were no significant differences (p-value = 0.095). a comparison between the data gathered in the same river both in the field (Hunzinger and Durrer, 2009) and generated with GIS (Bachmann, 2012) in the Schwartze Lütschine river, flooded in 2005.

The role of other factors in channel widening

None of the parameters listed below showed significant differences according to the hypothesis contrast tests (Kruskal-Wallis for vegetation, slope gradient and river morphology; Wilcoxon for the embankment). Corresponding boxplots and scatterplots available in the **Electronic Appendix**.

i) **Vegetation** (n=310)
ii) **Slope gradient** (n=1818)

iii) River embankment (n=20)
iv) River morphology (n=325)

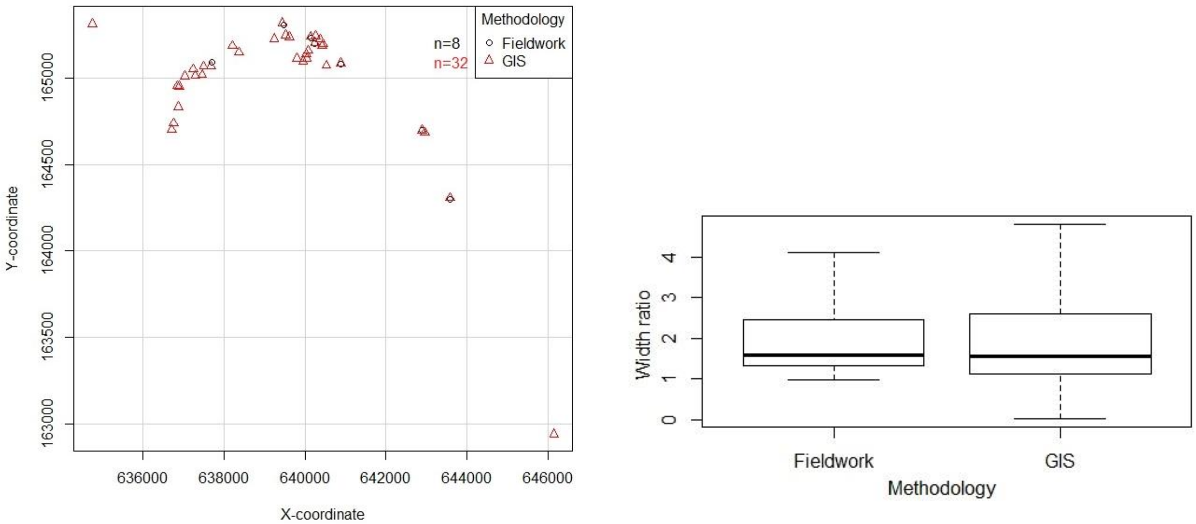

Figure 7. Left: scatterplot representing X against Y-coordinates by the methodology used in Schwartze Lütschine (Swiss Alps). Right: boxplot representing the width ratio against the type of methodology used (**Table 2**).

Table 3. Non-parametric hypothesis contrast tests' results.

Parameters	Test	W or chi-squared	p-value	Significant (p-value<0.05)
Lateral Confinement Index Methodology	Wilcoxon	181170	1,44E-01	No
Slope gradient Methodology	Wilcoxon	259670	1,64E-04	Yes
Stream power Methodology	Wilcoxon	6376	2,20E-16	Yes
Stream power index Methodology	Wilcoxon	124260	6,12E-05	Yes
Unit Stream Power Methodology	Wilcoxon	235900	2,20E-16	Yes
Wbf Methodology	Wilcoxon	246760	5,44E-13	Yes
Width ratio Methodology	Wilcoxon	364780	3,13E-03	Yes
Width ratio Return period class	Kruskal-Wallis	86,617	2,20E-16	Yes
Width ratio Region	Kruskal-Wallis	650,3	2,20E-16	Yes
Width ratio Slope class	Kruskal-Wallis	0,94118	6,25E-01	No
Width ratio	Kruskal-Wallis	4,8235	8,97E-02	No

Parameters	Test	W or chi-squared	p-value	Significant (p-value<0.05)
Vegetation class				
Width ratio River morphology	Kruskal-Wallis	5,2552	7,23E-02	No
Width ratio Catchment area class	Kruskal-Wallis	92,529	2,20E-16	Yes
Width ratio Embankment class	Wilcoxon	56	6,48E-01	No
Width ratio Lateral confinement class	Kruskal-Wallis	29,595	3,75E-07	Yes
Width before event Region	Kruskal-Wallis	45,713	2,83E-09	Yes
Slope gradient Lateral confinement class	Kruskal-Wallis	69,528	7,98E-16	Yes
Stream power index Lateral confinement class	Kruskal-Wallis	56,061	6,71E-13	Yes

DISCUSSION

Combining different approaches and methods to a wide array of different spatial scales is key for a successful monitoring and post-flood analysis of flash floods, due to the limited characterization of such events (Rinaldi *et al.*, 2016). Hydraulic controls alone are not adequate to explain channel widening (Hajdukiewicz *et al.*, 2016; Surian *et al.*, 2016). Clearly, other factors such as lateral confinement, channel slope, or percentage of reach length with artificial structures (Surian *et al.*, 2016) as well as the role of flow duration (Costa and O'Connor, 1995; Magilligan *et al.*, 2015) influence the geomorphic effects of floods (*i.e.* streambank erosion and channel widening). This study finds a significant correlation between the width ratio and other parameters, such as lateral confinement, catchment area and event return period. Others, such as those calculated (*i.e.* SP, USP, SPI) and the width before event, the artificial channeling or slope gradient-dependent parameters are susceptible to other parameters' value, thus, need additional study (**Table 3**).

- ***Data acquisition and difficulties***

As one of the fundamental objectives of this thesis was to provide an understanding of geomorphic indicators controlling channel widening during flood events, the database was prepared by gathering data from previous individual studies and further completed. In order to compare and analyse the compiled information, the dataset needed to be not only broad enough as to perform statistic tests to it, but as homogeneous as possible. This is the principal limitation to the presented data's reliability.

<u>Data availability and reliability</u>

Different authors had different goals for the same river and studied event, thus the provided data sometimes was not detailed enough (*e.g.* lack of spatial and/or temporal resolution) for the objectives of this study, or it didn't consider some of the key parameters of this study: width of the channel before the event, slope, coordinates, etc. Some of the parameters could be calculated based on the data available (*i.e.* unit stream power, stream power index, lateral confinement index, width ratio), but at times the most relevant ones sometimes were missing (*i.e.* there was no data on the width before the event in Lierza creek in North Italy, thus, lateral confinemet index could not be estimated), which made it necessary to discard studying some parameters of that river any further, as the data processing wouldn't be possible with so little information about the impacts of the event.

At times, it lacked before and exactly after event data, or information both collected in the field and in aerial photography is not available. This was needed for the comparison of data by methodology, and to estimate the affinity between data gathered at a certain site both in the field and subsequently completed with GIS analysis (*i.e.* only feasible for the 2005 floods in Switzerland). The 2013 and 2014 flood episodes affecting the Garona and Emme rivers were approached following the same process, although it is important considering whether all former works used pre- and post-flood data with comparable quality. Events in the same region were sometimes studied aiming different objectives, thus, most likely, practices might have been different and not necessarily equal to the ones used in this study.

Methodology used to compile data is a sensitive matter, as shown by the significant differences obtained when non-parametric tests were applied. GIS software made part of the data compilation more complex as, even though an advanced license was used, some of the tools needed to obtain relevant data were not available in the package, or the software misinterpreted the input data (*i.e.* it was necessary to assign IDs to each studied section and double-check manually that they were correctly ordered following the flow direction, which was not the case for Garona or Emme rivers). Therefore, downloading extensions, as Transects 2.0 (Ferreira, 2014), Fluvial Corridor toolbox (Roux *et al.*, 2015) or Polygon to Centerline tool (Dilts, 2015), was necessary. Even though some steps described in this thesis were inspired by Righini *et al.* (2017) in order to homogenize and reduce errors, there is not information concerning the methods used by other researchers nor it can be guaranteed that the data was collected in a similar way or by means of a less semi-automatic process. Therefore, results might be affected by the methodology used. Even if GIS software needed data verification, this method allowed to gather a myriad of information in much shorter time and, expectedly, of similar reliability.

As for the data acquired in the field (*i.e.* 2005 and 2011 flood episodes in Switzerland; Hunzinger and Durrer, 2009; Bachmann, 2012, respectively), it is critical to contemplate whether it was acquired immediately after the event, and the fact that there is a wide array of criteria that can be used when collecting data on site. It is worth paying special attention to whether field data is coherent with GIS data obtained in the same episode, this only demonstrable for the 2005 event (*e.g.* fieldwork data obtained by Hunzinger and Durrer, 2009, and GIS data generated by Bachmann, 2012): there were more GIS than fieldwork points, as the latter one depends on the accessibility to the point intended to measure. However, GIS-based interpretation of channel widening tends to be overestimated, as vegetation cover, artificial structures, or even insufficient image resolution make the process less accurate than fieldwork-gathered data, yet more homogeneous and comparable.

It is worth emphasizing that, as data was collected by different researchers in the different rivers (see previous works), most likely both different methodology and individual skills influenced the quality and comparability of the collected data.

Homogenization of parameters considered in different studies

Active channel, defined as the width of the functional channel and the eroded sediment bars in the river channel (*e.g.* Emme river, Garona river in this thesis) was used as it allowed to evaluate the bankfull width of the river, where the width of the channel was at its maximum, thus affected by erosion processes when the flood episode occurred.

In the case of the Garona River, the valley width was estimated based on the width of the ancient channel (aerial photography, 1956, ICGC [on line]) and the floodplain or lowest alluvial terrace altogether. In some cases, the floodplain does not exist because of entrenchment and lateral constraint (Victoriano *et al.*, 2016) and could not be identified in the aerial photographs, thus, discarded in that side of the river channel. Lateral confinement index was calculated based on the width of the channel before the event and the width of the valley. As some of the data compiled from previous works did not provide either one or another value, this parameter could not be estimated in many cases (Krapesch *et al.*, 2011; Hajdukiewicz *et al.*, 2016; Amponsah, 2017).

- Controlling factors

Channel widening observed during the flood events considered in this study is noticeably variable among regions. Moreover, the significance of other contemplated parameters (*i.e.* stream power index, confinement index, catchment area, flood magnitude, width before event) in river's response to a flash flood does not seem to be mediated by channel slope (**Table 3**; **Electronic Appendix**), contrary to what it was statistically demonstrated in Surian *et al.* or Comiti *et al.* (both from 2016; **Table 4** of this thesis). Significant differences were mainly observed as width ratio (Wr) was compared among the different regions, return periods (RT), catchment areas, methodology and, most importantly, lateral confinement (LC).

Table 4. Compilation of concluding controlling factors.

Reference	Main controlling factors
Krapesch *et al.*, 2011	Stream power, width before event, catchment area
Bachmann, 2012	Channel type, river morphology, vegetation cover, shear stress
Hooke, 2015	Return period/ flood magnitude
Nardi and Rinaldi, 2015	Vegetation cover, river morphology
Comiti *et al.*, 2016	Slope gradient (lateral confinement was not considered)
Hajdukiewicz *et al.*, 2016	Lateral confinement, channelling/artificial structures
Surian *et al.*, 2016	Stream power (slope-dependent), lateral confinement
Amponsah, 2017	Unit stream power, lateral confinement, river morphology, bed type
Righini *et al.*, 2017	Lateral confinement, unit stream power (width before event-dependent)
This project	LC, catchment area, RT, width before event, unit stream power

Changes in channel width: width ratio

As mentioned in Results, there is a significant difference in channel widening among regions, where rivers with larger widths before (Wbf) the floods showed lower width ratios (Wr). The variability is reduced, as well: regions presenting large variability in Wbf showed very little in Wr. This might be due to the fact that narrow channels tend to be unmanaged (*e.g.* lack of artificial structures) compared to the widest ones, as it was the case in the Carpathians.

Channel widening compared in function of the river' stream power index (SPI, **Electronic Appendix**), showed that Apennines presented lower SPI but higher width ratio, with very little dispersion, whereas the Pyrenees or the Alps displayed larger SPI for low width ratios, and a more disperse tendency. This could be due to the river management characteristics (*e.g.* if the river presents low SPI but large channel widening, this might not be due to the factors taking part in SPI calculus: slope gradient, catchment area and width before the event, but others, as lateral confinement).

Flood magnitude and channel widening

Opposite of what one may expect, frequent events (RT<50 years) presented significantly larger width ratios, with nearly twice as large variances compared to those of greater RT. However, this could be explained if rivers affected by frequent floods had a certain channel type (*i.e.* braided, in Carpathians), of a moderate confinement index. In order to get a more accurate idea, the comparison shall be done between rivers of the same cannel type, but affected by episodes of different magnitudes. Comparing width ratios against SPI by return period class (**Electronic Appendix**) allowed discerning that the pattern was very similar to the one by region, where Pyrenees corresponded to a frequent event, of a noticeable dispersion and Apennines and Alps to an extreme one. Wr against stream power (SP) and unit stream power (USP) showed similar dispersion.

Catchment area and channel widening

Rivers with both large and small catchment areas (>100km^2 and <10km^2, respectively) presented significantly larger Wr, as shown in **figure 5** (left), with an important data variance compared to small and moderate catchment areas. The first could be because there are more tributaries meeting the watercourse, hence, contributing with larger water discharges during the flood episode. This may as well suggest that rivers have a larger area in which to move laterally, although this depends on the river morphology, channel type, embankment, lateral constraint, presence of artificial structures, slope gradient, etc. Further analysis (*i.e.* plotting channel Wbf against the catchment area, or lateral confinement against catchment area, in order to check if watercourses of larger catchments were initially wider, as expected) needs to be done. Scatter plotting the width ratio against the unit stream power (USP) by catchment area class, it is noticed that small catchments (<10km^2) tend to have smaller USP despite the Wr, however, moderate to large catchment areas present small to intermediate Wr, with lower USP for larger catchment areas, yet equally dispersed in both cases.

Lateral confinement and channel widening

When representing width ratio against the lateral confinement (**Fig. 6**, left), rivers with higher confinement presented a similar channel widening to those moderately confined, yet both significantly lower than those reaches poorly confined. What is important noticing, though, is the distinctly larger variance displayed in rivers with low lateral confinement class compared to the proportionally lower variance in those moderately and highly confined. This result is also evident in the scatterplot representing the width ratio against the stream power index by lateral confinement class (**Fig. 6**, right) and Wr against USP (**Electronic Appendix**). This remarkable relationship suggests that this parameter might be one of the most decisively influencing geomorphic response to flash floods, which was previously demonstrated by other studies (Hajdukiewicz *et al.*, 2016; Surian *et al.*, 2016; Righini *et al.*, 2017; **Table 4** in this thesis).

Methodology used in data acquisition and channel widening

This is a concerning parameter in relation to the reliability of the studied data, thus, it is of vital importance to contrast the compiled information in seek of homogeneity. In the boxplot of **figure 7** (right) it is visually appreciated that width ratio is practically the same no matter what methodology was used when gathering data. However, non-parametric Wilcoxon test indicates significant differences, probably due to a larger variance in GIS generated data.

In the data reliability discussion section, it was mentioned that a comparison of field data against GIS data (**Electronic Appendix**) was carried out based on sections' geographic coordinates in order to discern whether the measured data was very different from the GIS data, and the test result was negative. However, this test was only possible to perform in a Swiss river affected during the 2005 flood, as no other study case included in the database was both studied in the field and with GIS. Even though this data was compiled by different researchers, thus, not necessarily explain the data coherence obtained when the same criteria is used, this would need a more complete dataset with similar cases in other watercourses in order to conclude whether the applied methods are significantly different at a local scale.

However, the scatterplot in **figure 7** (left), as well as those representing Wr against Wbf, USP or SPI by methodology class (**Electronic Appendix**), show a very similar tendency as the boxplots representing only the Wr against the methods: there is a larger dispersion in GIS-compiled data. This could be both due to the fact that GIS grants access to places where one cannot access in the field (*e.g.* more data availability in the case of GIS) and an individual skill-based induced error.

As mentioned in Methods, unit stream power and stream power index were calculated using the pre-flood channel width. Previous works (Krapesch *et al.*, 2011; Surian *et al.*, 2016; Amponsah, 2017; in **Table 4**) have proved that these hydraulic forces computed with channel width before a flood generally predict more accurately channel widening compared to using post- flood channel width instead. The fact that these parameters show a distribution alike to the Wr and Wbf is clearly explained as Wbf was considered when calculating the hydraulic forces abovementioned.

The role of other factors in channel widening

The corresponding graphs are included in the **Electronic Appendix**.

i) Vegetation

For frequent and maybe extraordinary floods, tree roots can help avoiding margin erosion. Nevertheless, in extreme flood events trees are easily ripped off, boosting margin erosion. This factor was scarcely available due to the data compilation process used in this thesis: no detailed data was provided in previous works, but a general estimation, therefore, this could not be properly considered in data analysis. However, the p-value= 0.0896 (**Electronic Appendix**), is only significant if we considered p-values <0.1. This suggests that it might be determinant if it's more thoroughly evaluated (Bachmann, 2012; Nardi and Rinaldi, 2015; in **Table 4**), although scatterplots of Wr against SP, SPI, USP and Wbf are rather disperse.

ii) Slope gradient

Slope gradient showed a very low significance in the overall data comparison (p-value= 0.624, **Electronic Appendix**), unlike what other studies suggested (Comiti *et al.*, 2016; Surian *et al.*, 2016; in **Table 4**).

Channel widening was not explained by the width before the event classified in different slope groups (**Tables 2** and **3**), as watercourses with lower slopes presented both larger initial widths and higher width ratios, and rivers with steeper slopes showed smaller initial widths and subsequent width ratios. It was also noticed that, the steeper the slope, the lower the width ratio and lateral confinement. Also, that for different slope values, the width ratio has a similar tendency.

This might be explained if we consider that either a) this parameter is very sensitive to measure, or b) channel widening has a higher dependence on other factors:

a) Slope measured in the field depends on three factors: the method used (*i.e.* total station, manual or semi-automatic), selection of sections to measure (*e.g.* length, choosing the upstream/ downstream/ segment containing the considered section), and accessibility in the field (*e.g.* to all sections or only a few of them, visibility). This parameter is important to consider, even though it is very sensitive, as it determines stream power, unit stream power, stream power index, etc.

b) It is probable that channel widening is decidedly determined by the lateral confinement, especially when the channel is entrenched or partially entrenched in bedrock, rather than the slope gradient, as they present a direct relationship, unlike width ratio against slope gradient.

There might be a third option, however, explained locally: the watercourse may be inclined to flowing straight when the water flows at high velocities, yet can adjust to the orography.

iii) River embankment

Few data were compiled on this factor; thus, the data did not show significant differences (Electronic Apendix). However, Hajdukiewicz *et al.* (2016; in **Table 4**) show a noticeable influence of artificial structures constraining partly or at all the river channel.

iv) River morphology

Local research (Bachmann, 2012; Nardi and Rinaldi, 2015; in **Table 4**) pointed this parameter out as a determinant one in channel widening. However, data seemed rather disperse and not significantly different (**Electronic Appendix**).

v) Hydraulic forces (USP, SPI, SP)

Despite the fact that some authors (Krapesch *et al.*, 2011; Surian *et al.*, 2016; Amponsah, 2017; Righini *et al.*, 2017; in **Table 4**) might have identified these factors as very relevant in channel widening, as they are estimated based on slope gradient, width before the event, catchment area, peak discharge, etc., they are conditioned by the influence of these parameters in the geomorphic response of rivers to flood events, therefore, no significant differences were observed (**Electronic Appendix**).

- Implications for flood hazard

Although some relationship of geomorphic response at catchment scale is usually evident, some issues are demanding and needed to be addressed. For example, the identification of the most significant variables and indicators related to geomorphic changes is a basic concern.

Besides a documentation of the flood episode, understanding how and to what extent it is possible to predict morphological response in similar catchments or in the same catchment for similar hydrometeorological events is a challenging matter. Important limitations make it extremely difficult to achieve a reliable prediction of possible geomorphic responses in apparently similar contexts.
Observations on channel changes such as widening are important, for example, for the correct interpretation of other field measurements or the identification of cross-sections that are not reliable for post-event field campaigns as they drastically changed the geometry during or after the peak stage. Additionally, feedback between channel processes are clear and may not be identified well if these features are not sufficiently analyzed. According to Rinaldi *et al.* (2016), a widening would cause the channel to cover the whole valley floor, which may result in the coupling of landslides, obstructing the channel and causing an induced flood episode, events that were not necessarily connected to the river system prior to the event. Tracking certain indicators may allow to explain, for instance, if a dam was constructed near the watercourse, and a change in the base level re-activated erosive processes in the headwaters.
Although, no significant statistical relationships were found between some hydraulic variables and the geomorphic response, relatively good regression models were obtained using confinement index as an explanatory variable. This was possible because data of different regions was considered and compared altogether, which leads to more robust conclusions that could be extrapolated and used in river and flood management. If data on lateral confinement, catchment area and unit stream power were, for instance, taken into account to predict the minimum morphological spatial demand of rivers during flash floods, and considered in hazards zone plans (*i.e.* estimating a minimal distance to the watercourses, where no urbanization was permitted), this would reduce potential loss due to erosion during high-magnitude floods.

CONCLUSIONS AND FUTURE RESEARCH

In the current thesis, a database of geomorphic and hydrologic characteristics of some selected study cases was confectioned. Subsequently, streambank erosion and channel widening were assessed in the selected study cases where data was adequately broad. Analysing these parameters provided an understanding of geomorphic indicators controlling bank erosion processes during high magnitude flood events. In other words, data on different flood events in varied watercourses was gathered and analysed, which provided better knowledge that would help estimating potential widening-related hazards during floods.
Through the data (n=2539) analysis, cases of river incised in bedrock (*e.g.* high lateral confinement index) and steep slope presented low width ratio. This can be explained based on the overall results obtained in this study, considering that slope is not the most relevant factor determining channel widening. However, in future research, if high confinement cases were excluded from the dataset and the rest were re-analyzed, or added other parameters that would evidence and help studying lateral confinement in rivers and its influence, perhaps this would indicate that other factors acted complementarily to the lateral confinement, or showed some interdependence.
It is of vital importance in river management and river monitoring to understand what factors condition river response to high magnitude flood episodes. A simplified approach to an

approximate estimation of the average and maximum extent of the widening expected during an extraordinary to extreme (return period >50-100years) episode in mountain basins could be based on the upper ranges for the observed width ratios, with the caution that the presented database is limited by the fact that data homogenization and reliability cannot be fully guaranteed, thus some parameters (*i.e.* vegetation cover, river morphology, embankment, slope gradient, presence of artificial structures) remain yet to be further explored.
Results presented in this study are conditioned by data dissimilarity. When data was not complete enough (*e.g.* present in a few rivers), the information it provided was only used aiming to understand local processes and data dispersion. In the future, an analysis of planimetric errors resulting from the visually-skilled interpretation and digitization processes, as well as determining whether the amount of changes in the measured parameters largely exceeds these errors. Parallel to the error analysis, in cases where dataset was large enough, yet not statistically significant, it could be treated as a confirmation that it necessary to work with rivers in more homogeneous areas, where the same parameters would be considered, yet the data correlation might be higher.
The investigation did not include floodplain's lithology, vegetation cover at a generic nor specific level, water flow velocity, precipitation distribution, etc. All these aspects might be of great use when it comes to explaining local variability, and might be applied when the study areas are homogeneous. Last, but not least, an important matter is the need to implement an overall analysis on the whole river catchments, although the flood event and its responses may concentrate only in some areas.

ACKNOWLEDGEMENTS

I wish to thank Annette Bachmann, Lukas Hunzinger, Dieter Rickenmann, Ernest Bladé, Bartłomiej Wyżga, Hanna Hajdukiewicz, Wiktoria Czech, and the Institut Cartogràfic i Geològic de Catalunya (ICGC) for the provided data. Thanks to M. Skalli, M. Condamines and N. Zanghi for having me at home back in Geneva.
I would like to express my gratitude for Andrés Díez Herrero, the initial brainstorm of ideas long before starting the project, and the inspiration for this thesis' topic. Thanks to my supervisors, Virginia Ruiz-Villanueva and Glòria Furdada, for their continuous guidance and valuable reviews; to my classmates, colleagues, professors, and all those who ever engaged in a geology-related debate, providing some critical sense to my initial lack of expertise and encouraging me to grow.

REFERENCES

Amponsah, W. (2017). Stream Power and Geomorphic Effects of Flash Floods. PhD Thesis, University of Padova. 166pp.

Bachmann, A. (2012). Ausmass und auftreten von seitenerosionen bei hochwasserereignissen. MSc Thesis, Universität Bern. Unpublished. 157pp. (In German)

Badoux, A., Böckli, M., Rickenmann, D., Rickli, C., Ruiz-Villanueva, V., Zurbrügg, S., & Stoffel, M. (2015). Large wood transported during the exceptional flood event of 24 July 2014 in the Emme catchment (Switzerland). In: Wood in world rivers. Proceedings of the third International Conference Wood in World Rivers 2015 - extended abstracts. Padova, Italy, pp.109–111.

Bagnold, R. A., 1977. Bed load transport by natural rivers. Water Resources Research, 13, 303–312.

Baker, V. R. (1988). Flood erosion. In: Flood Geomorphology. New York, USA: John Wiley & Sons, pp.1057–1071.

Bowen, M. W., & Juracek, K. E. (2011). Assessment of the geomorphic effects of large floods using streamgage data: the 1951 floods in eastern Kansas, USA. Physical Geography, 32(1), 52–77.

Buraas, E. M., Renshaw, C. E., Magilligan, F. J., & Dade, W. B. (2014). Impact of reach geometry on stream channel sensitivity to extreme floods. Earth Surface Processes and Landforms, 39(13), 1778–1789. https://doi.org/10.1002/esp.3562

Cavalli, M., Goldin, B., Comiti, F., Brardinoni, F., & Marchi, L. (2017). Assessment of erosion and deposition in steep mountain basins by differencing sequential digital terrain models. Geomorphology. 291, 4-16. http://doi.org/10.1016/j.geomorph.2016.04.009

CHE, Confederación Hidrográfica del Ebro (2008). Documentación Previa Para Su Análisis: Plan Hidrológico De La Cabecera Del Río Garona (V2.0). 141pp. (In Spanish)

CHE, Confederación Hidrográfica del Ebro (2013). Caudales horarios del río Garona el 18 de junio 2013 obtenidos con el modelo ASTER. Available at: http://www.chebro.es/ (last access: March 2017) (In Spanish)

CHE (Confederación Hidrográfica del Ebro), & MAPAMA (Ministerio de Agricultura, Alimentación y Medio Ambiente). (2014, March 10). Nota de prensa “De Pedro presenta las conclusiones del informe sobre las avenidas extraordinarias en el Garona con acciones para mejorar la gestión en estos episodios”, Vielha, pp. 1–8. (In Spanish)

Clément, P., & Piégay, H. (2003). Statistics and Fluvial Geomorphology. In: G. M. Kondolf & H. Piégay (Eds.), Tools in Fluvial Geomorphology. Hoboken, New Jersey, USA: John Wiley & Sons Ltd. ISBN: 047149142X, pp. 597–630.

Comiti, F., Righini, M., Nardi, L., Lucía, A., Amponsah, W., Cavalli, M., & Surian, N. (2016). Channel widening during extreme floods: how to integrate it within river corridor planning? In: INTERPRAEVENT, Lucerne, Switzerland, pp. 477–486.

Costa, J. E., & O’Connor, J. E. (1995). Geomorphologically effective floods. In: J. E. Costa, A. J. Miller, K. W. Potter, & P. Wilcock (Eds.), Natural and anthropogenic influences in fluvial geomorphology. Washington D.C.: Monograph (89), American Geophysical Union, pp. 45–56.

Crawley, M. J. (2013). The R Book. (M. J. Crawley, Ed.) (2nd ed.). Chichester, UK: John Wiley & Sons Ltd., 1072pp. http://doi.org/10.1007/s007690000247

Czuba, J. A., Magirl, C. S., Czuba, C. R., Curran, C. A., Johnson, K. H., Olsen, T. D., Kimball, H.K., & Gish, C. C. (2012). Geomorphic analysis of the river response to sedimentation downstream of Mount Rainier, Washington. Open File Report 2012-1242. Reston, Virginia, USA: U.S. Department of the Interior, U.S. Geological Survey (USGS), 134pp.

Dilts, T.E. (2015). Polygon to Centerline Tool for ArcGIS. University of Nevada Reno. Available at: http://www.arcgis.com/home/item.html?id=bc642731870740aabf48134f90aa6165 (last access: May 2017)

Ferreira, M. (2014). Transect Tool for ArcGIS 10. Available at: http://gis4geomorphology.com/stream-transects-partial/ (last access: May 2017)

García-Silvestre, M. (2015). L’avinguda de juny de 2013 al sector d’Era Bordeta - Les (Val d’Aran): efectes i dinàmica. BEng Thesis, Polytechnic University of Catalonia - University of Barcelona. 109pp. + 3 annexes. Unpublished. (In Catalan)

Godé, L. I., Gracia, A., De la Muñoza, C., Vera, M. A., Fleta, J., González, M., Jaquès, I., Micó, R., Oller, P., Pinyol, J., Pujal, E., Selfa, E., Tarragó, M., Trabal, L., Bastardós, C., & Oriach, R. (2013). Jornada “La gestió de les inundacions”: Síntesi de les ponències 27 i 28 de novembre 2013. Generalitat de Catalunya, Agència Catalana de l’Aigua, & Institut Geològic de Catalunya (Eds.), Barcelona, 138pp. (In Catalan)

Grove, J. R., Croke, J., & Thompson, C. (2013). Quantifying different riverbank erosion processes during an extreme flood event. Earth Surface Processes and Landforms, 38(12), 1393–1406. https://doi.org/10.1002/esp3386

Hajdukiewicz, H., Wyżga, B., Mikuś, P., Zawiejska, J., & Radecki-Pawlik, A. (2016). Impact of a large flood on mountain river habitats, channel morphology, and valley infrastructure. Geomorphology, 272, 55–67. https://doi.org/10.1016/j.geomorph.2015.09.003

Hooke, J. M. (2015). Variations in flood magnitude-effect relations and the implications for flood risk assessment and river management. Geomorphology, 251, 91–107. http://doi.org/10.1016/j.geomorph.2015.05.014

Hunzinger, L., & Durrer, S. (2009). Ereignisanalyse Hochwasser 2005: Seitenerosion. In: G. R. Bezzola & C. Hegg (Eds.), Ereignisanalyse Hochwasser 2005, Teil 2 - Analyse von Prozessen, Massnahmen und Gefahrengrundlgen. Bundesamt für Umwelt BAFU, Eidgenössische Forschungsanstalt WSL, Umwelt-Wissen Nr. 0825. Bern, pp. 1–159. (In German)

ICGC, Institut Cartogràfic i Geològic de Catalunya (1956). Orthophotographs of Catalonia, pixel size of 25cm [on line]. Barcelona: ICGC, 1956 [Downloaded: 09/02/2015]. Data property of ICGC under CC BY 4.0 license. URL: http://www.icc.cat/vissir3/index.html?QiQ0UlLNq

ICGC, Institut Cartogràfic i Geològic de Catalunya (2011). DEM of the Garona river basin, spatial resolution of 2m. Data property of ICGC under CC BY 4.0 license.

ICGC, Institut Cartogràfic i Geològic de Catalunya (2011). Orthophotographs of Catalonia, pixel size of 25cm [on line]. Barcelona: ICGC, 2011 [Downloaded: 09/02/2015]. Data property of ICGC under CC BY 4.0 license. URL: http://www.icc.cat/vissir3/index.html?QiQ0UlLNq

ICGC, Institut Cartogràfic i Geològic de Catalunya (2013). Orthophotographs of Vall d'Aran-Pallars, pixel size of 50cm [on line]. Barcelona: ICGC, 2013 [Downloaded: 09/02/2015]. Data property of ICGC under CC BY 4.0 license. URL: http://www.icc.cat/vissir3/index.html?QiQ0UlLNq

ICGC, Institut Cartogràfic i Geològic de Catalunya (2014). DEM of the Garona River basin, spatial resolution of 1m. Data property of ICGC under CC BY 4.0 license.

Knighton, A. D., 1999. Downstream variation in stream power. Geomorphology, 29, 293–306.

Krapesch, G., Hauer, C., & Habersack, H. (2011). Scale orientated analysis of river width changes due to extreme flood hazards. Natural Hazards and Earth System Sciences, 11(8), 2137–2147. https://doi.org/10.5194/nhess-11-2137-2011

Langhammer, L. (2010). Analysis of the relationship between the stream regulations and the geomorphic effects of floods. Natural Hazards, 54(1), 121–139. https://doi.org/10.1007/s11069-009-9456-2

Magilligan, F. J., Buraas, E. M., & Renshaw, C. E. (2015). The efficacy of stream power and flow duration on geomorphic responses to catastrophic flooding. Geomorphology, 228, 175–188. https://doi.org/10.1016/j.geomorph.2014.08.016

Ministerio de Agricultura y Pesca, Alimentación y Medio Ambiente, MAPAMA (2006). Cuencas hidrográficas de los principales ríos definidos en el artículo 3 de la Directiva Marco del Agua (DMA). Escala 1:25.000. MAPAMA. Available at: http://wms.mapama.es/sig/Agua/CuencasCauces/wms.aspx? (last accessed: May 2017)

Nardi, L., & Rinaldi, M. (2015). Spatio-temporal patterns of channel changes in response to a major flood event: The case of the Magra River (central-northern Italy). Earth Surface Processes and Landforms, 40(3), 326–339. https://doi.org/10.1002/esp.3636

Piégay, H., Darby, S. E., Mosselman, E., & Surian, N. (2005). A review of techniques available for delimiting the erodible river corridor: A sustainable approach to managing bank erosion. River Research and Applications, 21(7), 773–789. https://doi.org/10.1002/rra.881

QVI Inc., Quality Vision International Inc. (2010). ASCII to Raster conversion script for R: ETRS89 / UTM zone 31N - EPSG: 25831. Available at: http://epsg.io/25831 (last access: May 2017)

Rhoads, B. L. (1987). Stream power terminology. The Professional Geographer, 39(2), 189–195.

Rickenmann, D., Badoux, A., & Hunzinger, L. (2016). Significance of sediment transport processes during piedmont floods: The 2005 flood events in Switzerland. Earth Surface Processes and Landforms, 41(2), 224–230. https://doi.org/10.1002/esp.3835

Rickli, C., Böckli, M., Badoux, A., Rickenmann, D., Zurbrügg, S., Ruiz-Villanueva, V., & Stoffel, M. (2016). Schwemmholztransport während des Hochwasserereignisses vom 24 Juli 2014 im

Einzugsgebiet der Emme (Driftwood transport during the flood event of 24 July 2014 in the Emme river, Switzerland). Wasse, Energie, Luft, 108(3), 225–231. (In German)

Righini, M., Surian, N., Wohl, E., Marchi, L., Comiti, F., Amponsah, W., & Borga, M. (2017). Geomorphic response to an extreme flood in two Mediterranean rivers (northeastern Sardinia, Italy): Analysis of controlling factors. Geomorphology, 290, 184-199. http://doi.org/10.1016/j.geomorph.2017.04.014

Rinaldi, M., Surian, N., Comiti, F., & Bussetini, F. (2012). Guidebook for the evaluation of stream morphological conditions by the Morphological Quality Index (MQI) (Version 1.1). Roma: Istituto Superiore per la Protezione e la Ricerca Ambientale. Available at: http://www.isprambiente.gov.it/it/pubblicazioni/manuali-e-linee-guida/guidebook-for-the-evaluation-of-stream (last access: May 2017)

Rinaldi, M., Surian, N., Comiti, F., & Bussettini, M. (2013). A method for the assessment and analysis of the hydromorphological condition of Italian streams: The Morphological Quality Index (MQI). Geomorphology, 180–181, 96–108. https://doi.org/10.1016/j.geomorph.2012.09.009

Rinaldi, M., Surian, N., Comiti, F., Bussettini, M., Nardi, L., & Lastoria, B. (2015). Idraim: A methodological framework for hydromorphological analysis and integrated river management of Italian streams. In: Engineering Geology for Society and Territory - Volume 3: River Basins, Reservoir Sedimentation and Water Resources, pp. 301–304. http://doi.org/10.1007/978-3-319-09054-2_62

Rinaldi, M., Amponsah, W., Benvenuti, M., Borga, M., Comiti, F., Lucía, A., Marchi, L., Nardi, L., Righini, M., & Surian, N. (2016). An integrated approach for investigating geomorphic response to extreme events: Methodological framework and application to the October 2011 flood in the Magra River catchment, Italy. Earth Surface Processes and Landforms, 41(6), 835–846. https://doi.org/10.1002/esp.3902

Rohatgi, A. (2015). Web Plot Digitizer. Distributed under GNU AGPL v3 license. Available at: http://arohatgi.info/WebPlotDigitizer/app/

Ros San Martin, G. (2015). Transport de sediments a Salardú durant la riuada de juny 2013. BEng Thesis, Polytechnic University of Catalonia. Unpublished. 66pp. (In Catalan)

Roux, C., Alber, A., Bertrand, M., Vaudor, L., & Piégay, H. (2015). "Fluvial Corridor": A new ArcGIS toolbox package for multiscale riverscape exploration. Geomorphology, 242, 29–37. https://doi.org/10.1016/j.geomorph.2014.04.018

Schumm, S. A. (1977). The fluvial system. New York, USA: John Wiley & Sons. 338pp.

Surian, N., Righini, M., Lucía, A., Nardi, L., Amponsah, W., Benvenuti, M., Borga, M., Cavalli, M., Comiti, F., Marchi, L., Rinaldi, M., & Viero, A. (2016). Channel response to extreme floods: Insights on controlling factors from six mountain rivers in northern Apennines, Italy. Geomorphology, 272, 78–91. https://doi.org/10.1016/j.geomorph.2016.02.002

Thompson, C., & Croke, J. (2013). Geomorphic effects, flood power, and channel competence of a catastrophic flood in confined and unconfined reaches of the upper Lokyer valley, southeast Queensland, Australia. Geomorphology, 197, 156–169.

Victoriano, A. (2014). Reconstrucción y análisis geomorfológico de la avenida de junio de 2013 entre Arties y Vielha (Val d'Aran): estudio del riesgo residual y dinámica del Garona. MSc Thesis, University of Barcelona. 25pp. + 6 annexes. Available at: http://hdl.handle.net/2445/57067 (last access: February 2017) (In Spanish)

Victoriano, A., García-Silvestre, M., Furdada, G., & Bordonau, J. (2016). Long-term entrenchment and consequences for present flood hazard in the Garona River (Val d'Aran, Central Pyrenees, Spain). Natural Hazards and Earth System Sciences, 16(9), 2055–2070. https://doi.org/10.5194/nhess-16-2055-2016